Experimental test of a newly developed single-moderator, multi-detector, directional neutron spectrometer in reference monochromatic fields from 144 keV to 16.5 MeV

R. Bedogni [a,*], J.M. Gómez-Ros [a,b], A. Pola [c,d], D. Bortot [c,d], A. Gentile [a], M.V. Introini [c,d], B. Buonomo [a], M. Lorenzoli [c,d], M. Mazzitelli [a], D. Sacco [a,e]

[a] INFN – LNF, via E. Fermi n. 40, 00044 Frascati (Roma), Italy
[b] CIEMAT, Av. Complutense 40, 28040 Madrid, Spain
[c] Politecnico di Milano, Dipartimento di Energia, via La Masa 34, 20156 Milano, Italy
[d] INFN – Milano, Via Celoria 16, 20133 Milano, Italy
[e] INAIL – DPIA, Via di Fontana Candida n.1, 00040 Monteporzio Catone, Italy

ARTICLE INFO

Article history:
Received 24 December 2014
Received in revised form
2 February 2015
Accepted 2 February 2015
Available online 11 February 2015

Keywords:
Neutron spectrometry
Neutron dosimetry
CYSP
NESCOFI@BTF
NEURAPID
Directional spectrometry

ABSTRACT

A new directional neutron spectrometer called CYSP (CYlindrical SPectrometer) was developed within the NESCOFI@BTF (2011–2013) collaboration. The device, composed by seven active thermal neutron detectors located along the axis of a cylindrical moderator, was designed to simultaneously respond from the thermal domain up to hundreds of MeV neutrons. The new spectrometer condenses the performance of the Bonner Sphere Spectrometer in a single moderator; thus requiring only one exposure to determine the whole spectrum. The CYSP response matrix, determined with MCNP, has been experimentally evaluated with monochromatic reference neutron fields from 144 keV to 16.5 MeV, plus a ^{252}Cf source, available at NPL (Teddington, UK). The results of the experiment confirmed the correctness of the response matrix within an overall uncertainty of $\pm 2.5\%$. The new active spectrometer CYSP offers an innovative option for real-time monitoring of directional neutron fields as those produced in neutron beam-lines.

1. Introduction

New instruments for real-time spectrometric monitoring of neutron fields are becoming available to the scientific community, as those arising from the research of the NESCOFI@BTF and NEURAPID international collaborations [1]. Two devices were studied and developed, both based on array of active thermal neutron detectors embedded in a single moderator: SP^2 and CYSP. Both condense the functionality and performance of the extended range Bonner Sphere Spectrometer [2] in a single device, but their direction response was deliberately designed to be sharply different. The SP^2 exhibits isotropic response, due to the spherical shape, and is especially useful for radiation protection monitoring [3–5]. By contrast the CYSP has directional response, being similar in design to a long counter [6], but multiple thermal neutron detectors at different depths are used instead of a unique axial thermal neutron counter. Similarly to the long counter, the CYSP has a collimator to select the direction. Neutrons coming from different directions are absorbed in the lateral protecting structure, formed by polyethylene and borated plastic. The directional response, together with the real-time reading and the extended energy interval (from thermal energies up to hundreds of MeV), make the CYSP highly attractive for experiments where a continuous spectrum monitoring along a given direction is desired, such as the studies of angle-dependent (particle, n) reactions. None of the existing beam-monitor systems, even the newly proposed ones [7–10], show all mentioned functionalities together.

A detailed description of the CYSP design, achieved through extensive Monte Carlo simulation, is given elsewhere [11]. The same reference presents the simulated response matrix of the device, intended as the reading of each thermal neutron detector per unit incident fluence as a function of the neutron energy. This work focuses on the test of the active prototype, equipped with TNPD type thermal neutron detectors [12,13] developed in the NESCOFI@BTF and NEURAPID projects.

The CYSP prototype was exposed in monochromatic reference neutron fields of 0.144, 0.565, 2.0, 3.5, 5.0 and 16.5 MeV available at NPL (Teddington, UK). This experiment allowed calibrating the spectrometer and estimating the accuracy of the simulated response matrix in the low-energy domain (E < 20 MeV).

* Corresponding author.
E-mail address: roberto.bedogni@lnf.infn.it (R. Bedogni).

2. The CYSP spectrometer and its response

According to the final design described in previous work [11] and sketched in Fig. 1, CYSP is a HDPE cylinder with overall diameter 50 cm and total length 65 cm. The dimensions of the cylinder as well as the location of detectors have been chosen to maximize the "spectrometric capability" of the device, i.e. the degree of differentiation between the response functions associated to different detector positions. The collimator (label 1 in Fig. 1) is 30 cm in length and its collimating hole (label 2), 16 cm in diameter, is covered by 5 mm of borated plastic SWX-238 (label 3, www.shieldwerx.com). The seven thermal neutron detectors, located along the cylindrical axis, are contained in a HDPE capsule (20 cm in diameter, 30 cm in length). An external shield made of 5 mm of SWX-238 (label 3) plus 15 cm of HDPE (label 6) protects the sensitive capsule from lateral contributions over a broad energy range. A 1 cm thick, 20 cm in diameter, lead disk (label 4), has been inserted between 6th and 7th positions to increase the response to high-energy neutrons. The distance between two adjacent detector cavities is 2 cm (centre to centre). The seven detectors are located at depths 4, 6, 8, 10, 12, 14 and 21 cm from the end of the collimator. The latter is located under the 1-cm lead filter.

Label 5 symbolizes eight cylindrical air cavities, 1 cm in diameter, designed to enhance neutron streaming towards the deeper detectors.

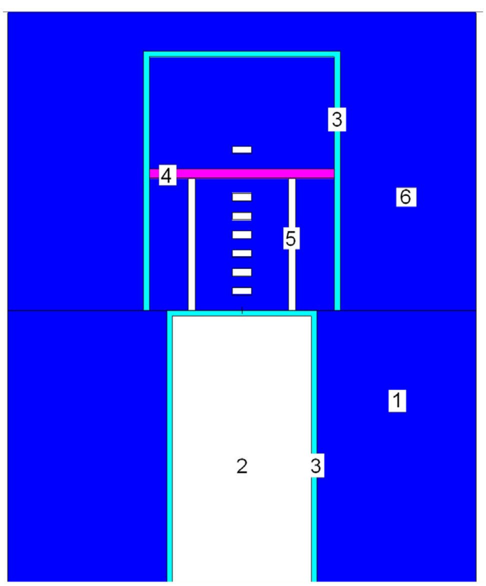

Fig. 1. Cross cut at mid-plane of the CYSP.

The different parts of the CYSP prototype are shown in Fig. 2. Left-top: the whole device separated into collimator and detector capsule plus shielding. Left-bottom: half of the capsule, with detector cavities and lead disk in evidence. Right: the detector capsule with the SWX-238 wrapping, and half of the HDPE shielding. The air penetrations are visible.

As explained in Refs. [12,13], the thermal neutron detectors developed for CYSP are 1-cm^2 windowless p-i-n diodes made sensitive to thermal neutrons through deposition of about 30 μm of ^{6}LiF on the sensitive face. Their special name is TNPD (thermal neutron pulse detector). Their response to thermal neutrons (in terms of counts per unit conventional thermal fluence) is about 0.03 cm^2. To account for small unavoidable detector-to-detector differences (in the order of 3%), every detector was individually calibrated at the INFN-LNF thermal neutron cavity [14].

The response matrix of the CYSP, $M_i(E)$ (units cm^2), shown in Fig. 3, was obtained as a result of an extensive Monte Carlo simulation campaign described in Ref. [11]. Other details, such as the capability of rejecting neutrons coming from unwanted directions, are addressed in the same paper. The response matrix was obtained by simulating an irradiation with a uniform parallel neutron beam having diameter 50 cm (the same diameter of the CYSP), and directed towards the collimator entrance (bottom to top in Fig. 1). $M_i(E)$ is the number of (n,γ) capture events in the ^{6}Li of the detector converter, per unit incident neutron fluence, as a function of the measurement point and of the neutron energy. Pedix "i", with $i=1,\ldots,7$, denotes the measurement position (depth increases with i).

As expected, the response maximum shifts towards higher energies as i increases. Whilst the responses of positions 1 to 5 show a clear maximum then decrease, that of position 7 monotonically increases with energy, by effect of the Pb filter. Interestingly, the effect of the lead above 10 MeV also extends to other positions that may be reached by thermalized secondary neutrons from (n, xn) reactions in the lead. Such a response increase in the 10–100 MeV region does not exist in pure polyethylene moderators, such as conventional Bonner Spheres [15] of any diameter. For this experiment CYSP was not equipped to see thermal neutrons because the studied monochromatic beams were all epithermal. Nevertheless, an un-moderated TNPD placed at the end of the collimator would certainly be suited to measure thermal neutrons present in the original field.

Because not all the neutron capture events in the LiF radiator produce measurable signals in the diode, the CYSP count profile per unit fluence, $C_i(E)$, will be lower than the corresponding simulated quantity $M_i(E)$. The ratio between the observed and expected counts is hereafter called *spectrometer calibration factor*, F. This number is lower than 1. If the simulated response well approximates the real spectrometer response, F does not depend on the measurement position and from the neutron energy. Its degree of constancy, when

Fig. 2. Different parts of the CYSP prototype.

the measurement position and the energy vary, can be used to estimate the "overall accuracy" of the simulated CYSP response matrix in the studied energy range.

For every monochromatic energy used in this experiment, and for every measurement position, an estimation of the calibration factor $F_{i,E}$ (where i denotes the measurement position and E the mono-chromatic energy) was experimentally derived. Information about the accuracy of the simulated response matrix was obtained from the distribution of the $F_{i,E}$ values.

3. Irradiation conditions

The irradiation tests took place from 28th to 31th October 2013 in the low-scatter irradiation room of NPL, using the Neutron Metrology Group 3.5 MV Van de Graaff accelerator. The exploited reactions were ^{7}Li(p,n), T(p,n), D(d,n) and T(d,n). All measurements were done at 0° from the neutron emitting target except the 3.5 MeV, where the 70° angle was used. The distance from target to instrument front face was 2 m. The shadow-cone technique was used to subtract the air- and room-scatter contribution to the spectrometer readings. Only the 3.5 MeV irradiation was performed without measurement of the air- and room-scatter components, so that the reference fluence for this beam was provided with slightly larger uncertainty. In the case of 16.5 MeV beam, additional measurements were needed to account for extra neutrons coming from the titanium substrate and the gold backing of the tritium target. These were performed by irradiating a "blank" target, identical to the tritied one except for the absence of tritium, again using the shadow-cone technique. The reference value of monochromatic neutron fluence delivered to the reference point (CYSP front face) was known through measurements with the Standard NPL long counter plus a suite of permanent monitor instruments. The main characteristics of the used beams are summarized in Table 1. It should be underlined that the "target scatter fraction", provided by NPL on the basis of Monte Carlo calculations, is constituted by neutrons with lower energy than the monochromatic one. Nevertheless, since the long counter used to determine the reference fluence has flat energy dependence of the fluence response, the result is a slightly overestimated value of the reference fluence. This was taken into account in data analysis.

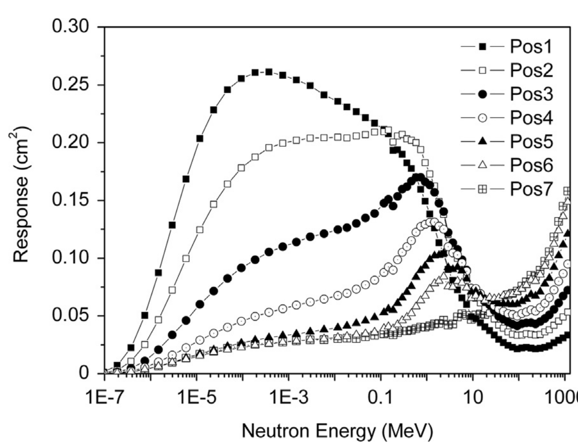

Fig. 3. The response matrix of the CYSP under irradiation with a parallel beam with diameter 50 cm.

An additional calibration of the CYSP was performed using a reference ^{252}Cf source (fluence average energy 2.13 MeV), placed at 2 m distance from the device front face, using the shadow-cone technique.

4. Results of the irradiation tests

For a given monochromatic irradiation, seven estimations (one per detector) of the CSYP calibration factor were derived as follows:

$$F_i = \frac{(C_{i,tot}/\Phi_{tot}) - (C_{i,cone}/\Phi_{cone})}{M_i} \times \text{TS} \quad i = 1, \ldots, 7 \qquad (1)$$

The symbols in Eq. (1) represent:

- $C_{i,tot}$the counts in the ith position in the total field irradiation.
- $\Phi_{tot}$the monochromatic reference neutron fluence delivered at the reference point (CYSP front face) during the total field irradiation (unit: cm^{-2}).
- $C_{i,cone}$the counts in the ith position in the irradiation with shadow cone.
- $\Phi_{cone}$the monochromatic reference neutron fluence that would be delivered at the reference point (CYSP front face) during the irradiation with shadow cone, in absence of shadow-cone (unit: cm^{-2}).
- TSthe target-scatter fraction as provided by NPL, in terms of fraction of total the fluence.
- $\tilde{M}_i$the expected number of neutron capture reactions in the (n,α) converter of the TNPD located at the ith position, per unit fluence at the reference point, when the neutrons are emitted by a point source (the target) located at 2 m from the CYSP front face. These considerations are relevant for this calculation:
  1. Although the response matrix of a device is normally derived under parallel beam condition, a realistic irradiation scenario with a point source at 2 m was needed in this case, because the CYSP dimensions were not negligible with respect to the irradiation distance.
  2. A realistic energy distribution, including the target-scatter contribution (Monte Carlo spectra provided by NPL), was used for modelling the source term.

In the case of the 3.5 MeV beam no shadow cone irradiation was performed, so that a larger uncertainty was assigned to the reference fluence to compensate the absence of the C_{cone}/Φ_{cone} term.

Table 1
The main characteristics of the used beams.

Nominal monochromatic energy (MeV)	Full width of energy distribution (MeV)	Reaction used	Measurement Angle	Typical fluence rate at nominal Monochromatic Energy (cm^{-2} s^{-1})	Standard uncertainty on reference fluence at reference point	Target scatter fraction (% of the total fluence)
144.4	10.3	^{7}Li(p,n)	0°	100	± 2.3%	0.9%
565.1	6.8	^{7}Li(p,n)	0°	320	± 2.3%	0.6%
2000.2	82	T(p,n)	0°	440	± 2.3%	1.9%
3493	52	D(d,n)	70°	26	± 4.6%	3.5%
5000	121	D(d,n)	0°	140	± 3.2%	0.8%
16,500	456	T(d,n)	0°	110	± 2.5%	3.0%

Table 2
Estimations of the CYSP calibration factor, $F_{i,E}$, from different monochromatic energy plus the ^{252}Cf and for the seven measurement positions.

	144 keV	565 keV	2 MeV	3.5 MeV	5.0 MeV	16.5 MeV	^{252}Cf
Position 1	0.195	0.200	0.204	0.196	0.202	0.214	0.201
Position 2	0.198	0.202	0.213	0.201	0.206	0.205	0.206
Position 3	0.194	0.196	0.203	0.193	0.193	0.194	0.195
Position 4	0.191	0.201	0.206	0.188	0.199	0.193	0.197
Position 5	0.189	0.199	0.204	0.184	0.194	0.190	0.196
Position 6	0.201	0.203	0.214	0.190	0.199	0.203	0.202
Position 7	0.182	0.210	0.214	0.199	0.199	0.204	0.207
F_E	0.194 ± 0.008	0.200 ± 0.006	0.207 ± 0.007	0.193 ± 0.011	0.199 ± 0.008	0.199 ± 0.010	0.200 ± 0.005

For the 16.5 MeV beam, two additional terms were included in Eq. 1 to account for the *blank target* and *black target with cone* irradiations.

The $F_{i,E}$ values experimentally obtained are reported in Table 2 for every monochromatic energy plus the ^{252}Cf source and for the seven detectors.

Uncertainties on the single $F_{i,E}$ values vary from ±3% to ±5% (one s.d.), given by the sum in quadrature of the uncertainty contributions from counting (typically less than ±1%), reference fluence (±2% to ±3% depending on the beam energy), device positioning (±0.2%), target scatter fraction (±0.2% to ±1%). For the 3.5 MeV beam uncertainties are in the order of ±5%, mainly due to the contributions from fluence (±4.6%) and scatter fraction (±1.4%).

The best estimation of the calibration factor was derived for every energy, using the inverse square of uncertainty as weighting factors. This corresponds to F_E, the last line of Table 2. Taking uncertainties into account, the F_E estimations from monochromatic beams are inter-compatible. The global calibration factor, F, was then obtained by a weighted average of the F_E values from monochromatic beams. Its numerical value is F=0.200 ± 0.005 (±2.5%), which coincides with the calibration factor obtained with the ^{252}Cf source and reported in Table 2. The ±2.5% figure can be regarded as an estimation of the "overall uncertainty" of the simulated response matrix for the investigated energy range.

In Figs. 4 and 5 the CYSP experimental counts per unit fluence, corrected for room-, air- and target-scatter (See Eq. 2), is compared with its "expected" value $F \cdot \tilde{M}_i$, i.e. the product of the global calibration factor F and the simulated response.

$$C_{i,corrected} = \left[\frac{C_{i,tot}}{\Phi_{tot}} - \frac{C_{i,cone}}{\Phi_{cone}}\right] \times TS \tag{2}$$

Uncertainty bars for the "expected" curves in Figs. 4 and 5 are the quadratic combination of the reference fluence uncertainty and the response matrix overall uncertainty, now estimated as ±2.5%.

The plots confirm that the simulated response matrix satisfactorily predicts the experimental spectrometer response for all investigated neutron energies. It should be noted that the profile for the ^{252}Cf source differs from that of the 2 MeV beam, even though their average energy is roughly the same. The profile maximum shifts at deeper positions within the CYSP as the energy increases. These are indications of the spectrometric capability of the device.

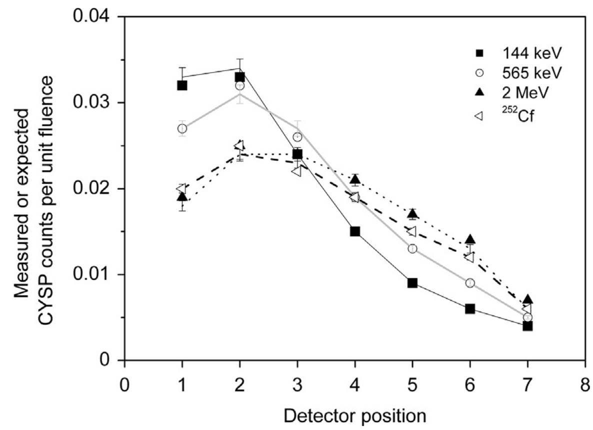

Fig. 4. CYSP experimental counts per unit fluence corrected for room-, air- and target-scatter (symbols), compared with their "expected" values (Lines) for 144 keV, 565 keV, 2.0 MeV and ^{252}Cf.

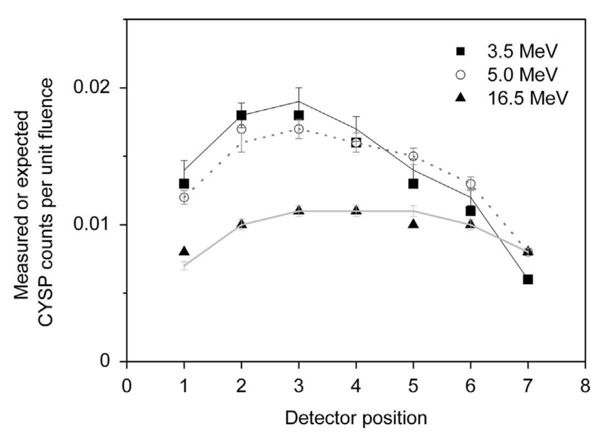

Fig. 5. CYSP experimental counts per unit fluence corrected for room-, air- and target-scatter (symbols), compared with their "expected" values (Lines) for 3.5 MeV, 5.0 MeV and 16.5 MeV beams.

5. Conclusions

CYSP (CYlindrical SPectrometer) is a prototypal neutron spectrometer with directional response. It consists of seven active thermal neutron detectors, obtained by depositing an adequate ^{6}LiF layer on 1-cm^2 p-i-n diodes, embedded in a complex polyethylene structure with an internal 1 cm thick lead shell. This instrument may serve as a real-time spectrometric monitor in neutron producing facilities where the directional information is relevant, such as neutron beams from targets. Relevant properties of CYSP are the sharply directional response up to hundreds of MeV neutrons and the ability to determine the whole spectrum in only one exposure. On the basis of the experiment with reference fields from 144 keV to 16.5 MeV described here, the theoretical response matrix of CYSP is able to predict the spectrometer experimental response within ±2.5%. A further experiment will be performed in the future to confirm the measured calibration factor at higher energies. Prior to its practical use in neutron facilities, CYSP will be also tested to investigate its performance in sharply pulsed fields. However, following the same computational approach adopted for the SP^2 spectrometer [3]; it can be foreseen that CYSP will accurately measure neutron pulsed fields up to at least 1 μSv/pulse. As far as the radiation damage aspects are concerned, the TNPD reading remains correct up to $> 10^{12}$ cm^{-2} (thermal) [12], whilst damage tests in very intense fast neutron fields are planned. For use beyond these limits, the 1-cm^2 Silicon detectors could be replaced by smaller and more radiation resistant SiC- or diamond-based detectors.

As it can be concluded from the results discussed above, CYSP is initiating a new generation of directional monitors for neutron producing facilities, able to continuously control the beam not only in terms of fluence rate, but also in terms of energy distribution over more than ten decades in energy.

Acknowledgements

This work has been supported by projects NESCOFI@BTF and NEURAPID from INFN-Italy (Commissione Scientifica Nazionale 5), and FIS2012-39104-C02 (MINECO, Spain). The staff of the NPL Neutron metrology Group is greatly acknowledged.

References

[1] R. Bedogni, J.M. Gómez-Ros, D. Bortot, A. Pola, M.V. Introini, A. Esposito, A. Gentile, G. Mazzitelli, B. Buonomo, Radiation Protection Dosimetry 161 (2014) 37.
[2] D.J. Thomas, Radiation Measurements 45 (2010) 1178.
[3] R. Bedogni, D. Bortot, B. Buonomo, A. Esposito, J.M. Gómez-Ros, M.V. Introini, M. Lorenzoli, A Pola, D Sacco, Nuclear Instruments and Methods in Physics Research, Section A 767 (2014) 159.
[4] R. Bedogni, J.M. Gomez-Ros, A. Pola, M.V. Introini, D. Bortot, A. Gentile, A. Esposito, G. Mazzitelli, B. Buonomo, L. Quintieri, L. Foggetta, Nuclear Instruments and Methods in Physics Research, Section A 714 (2013) 110.
[5] J.M. Gomez-Ros, R. Bedogni, M. Moraleda, A. Esposito, A. Pola, M.V. Introini, G. Mazzitelli, L. Quintieri, B. Buonomo, Nuclear Instruments and Methods in Physics Research, Section A 677 (2012) 4.
[6] H. Tagziria, D.J. Thomas, Nuclear Instruments Methods in Physics Research, Section A 452 (2000) 470.
[7] L. Giacomelli, M. Rebai, E. Perelli Cippo, M. Tardocchi, A. Fazzi, C. Andreani, A. Pietropaolo, C.D. Frost, N. Rhodes, E. Schooneveld, G. Gorini, AIP Conference Proceedings 1442 (2012) 305.
[8] F. Murtas, G. Croci, A. Pietropaolo, G. Claps, C.D. Frost, E. Perelli Cippo, D. Raspino, M. Rebai, N.J. Rhodes, E.M. Schooneveld, M. Tardocchi, G. Gorini, Journal of Instrumentation 7 (2012) 7021.
[9] A. Smirnov, A. Pietropaolo, A. Prokofiev, E. Rodionova, C. Frost, S. Ansell, et al., Nuclear Instruments and Methods in Physics Research, Section A 687 (2012) 14.
[10] R. Bedogni, A. Esposito, C. Andreani, R. Senesi, M.P. De Pascale, P. Picozza, et al., Nuclear Instruments and Methods in Physics Research, Section A 612 (2009) 143.
[11] J.M. Gómez-Ros, R. Bedogni, D. Bortot, B. Buonomo, A. Esposito, A. Gentile, M. Lorenzoli, M.V. Introini, G. Mazitelli, M. Moraleda, A. Pola, D. Sacco, Nuclear Instruments and Methods in Physics Research, Section A (2015) (Submitted for publication).
[12] A. Pola, D. Bortot, M.V. Introini, R. Bedogni, A. Gentile, A. Esposito, J.M. Gómez-Ros, E. Passoth, A. Prokofiev, Radiation Protection Dosimetry 161 (2014) 229.
[13] R. Bedogni, D. Bortot, A. Pola, M.V. Introini, M. Lorenzoli, J.M. Gómez-Ros, D. Sacco, A. Esposito, A. Gentile, B. Buonomo, M. Palomba, A. Grossi, Nuclear Instruments and Methods in Physics Research Section A 780 (2015) 51.
[14] R. Bedogni, D. Bortot, A. Pola, M.V. Introini, A. Gentile, A. Esposito, J.M. Gómez-Ros, M. Palomba, A. Grossi, Radiation Protection Dosimetry 161 (2014) 241.
[15] R. Bedogni, P. Ferrari, G. Gualdrini, A. Esposito, Radiation Measurements 45 (2010) 1201.